ON MULTI–SCALE CONCEPTS FOR MULTI–DIMENSIONAL CONSERVATION LAWS

Birgit Gottschlich–Müller[1], Siegfried Müller
Institut für Geometrie und Praktische Mathematik
RWTH Aachen
Templergraben 55
52056 Aachen, Germany

SUMMARY

In 1993, Ami Harten developed a concept to reduce the computational costs of finite volume schemes applied to hyperbolic conservation laws. It is based on a multi–scale decomposition of discrete data. By this decomposition, singularities in the flow field are detected. In the present work, we introduce a general multi–scale concept for discrete data. It is essentially based on prolongation and restriction matrices as known from multigrid theory. Two different concepts are presented how to determine the transfer matrices. The first one is based on Harten's general framework [H96] applied to cell averages. The second strategy examined by Carnicer, Dahmen and Peña [CDP] is based on bi–orthogonal wavelets. The relation between the two concepts is presented.

Numerical calculations for the rotational symmetric Euler equations are presented. We consider the unsteady shock focussing problem. The results show a significant reduction in computational time.

INTRODUCTION

In this paper we consider partial differential equations of the form

$$\frac{\partial\, u(t,\mathbf{x})}{\partial\, t} + \sum_{m=1}^{d} \frac{\partial\, f_m(u(t,\mathbf{x}))}{\partial\, x_m} = s(\mathbf{x}, u(t,\mathbf{x})), \qquad 0 < t < T,\ \mathbf{x} \in \Omega, \tag{1}$$

where $T > 0$ and $\Omega \in \mathrm{IR}^d$ are fixed. Systems of this type are called *conservation laws*. Here, $u : \Omega \to \mathrm{IR}$ is the conservative quantity, $f_m : \mathrm{IR} \to \mathrm{IR}$ the flux in the m–th coordinate direction and $s : \mathrm{IR} \to \mathrm{IR}$ the source term. In order to ensure a unique solution, an initial condition

$$u(0,\mathbf{x}) = u_0(\mathbf{x}), \qquad \mathbf{x} \in \Omega, \tag{2}$$

[1]This author is supported by the German Research Establishment in the Graduiertenkolleg "Transport Processes in Hypersonic Flow" at the RWTH Aachen.

has to be imposed. In physical meaningful applications, boundary conditions of the form

$$g(u(t,\mathbf{x}), u_{\mathbf{x}}(t,\mathbf{x})) = 0, \qquad 0 \le t \le T,\ \mathbf{x} \in \partial\Omega \tag{3}$$

are also required.

It is well known that a smooth solution u of (1, 2) exists in general only for small times T even if u_0 is smooth. Due to the nonlinearity of the flux, discontinuities may develop which results in the "break down" of the differentiable solution. From a physical point of view, these discontinuities are reasonable and should be admissible for a solution of (1, 2). Therefore, a weak formulation of (1) is introduced, namely

$$\int_V u(t+\tau,\mathbf{x})\, dV = \int_V u(t,\mathbf{x})\, dV - \int_t^{t+\tau}\int_\Gamma \langle \mathbf{f}(u(s,\mathbf{x})), \mathbf{n}(\mathbf{x})\rangle\, d\Gamma ds + \int_t^{t+\tau}\int_V s(\mathbf{x}, u(s,\mathbf{x}))\, dV\, ds \tag{4}$$

for all $V \subset \mathrm{IR}^d$ and $[t, t+\tau] \subset \mathrm{IR}_0^+$ (cf. [L]) with the flux vector $\mathbf{f} = (f_1, \ldots, f_d)^T$, the boundary $\Gamma := \partial V$ and the related outer normal $\mathbf{n}$. A function u fulfilling (4, 2) is called *weak solution*.

By equation (4) the class of *finite volume schemes* can be derived. For this purpose, we discretize the continuum $\Omega \times [0,T]$ in space and time. In the following, we decompose Ω by

$$\Omega = \bigcup_{j\in I} V_j, \qquad \partial V_j = \bigcup_{m=1}^{P_j} \Gamma_{m,j},$$

where the boundary of the cell V_j consists of $(d-1)$–dimensional faces $\Gamma_{m,j}$. By P_j we denote the number of faces corresponding to V_j, which is bounded for all volumes by some integer $P < \infty$. The temporal grid is uniformly discretized by $t_n = \tau\, n,\ \tau := T/N,\ N \in \mathrm{IN}$. Then, equation (4) takes the form

$$\hat{u}_j^{n+1} = \hat{u}_j^n - \lambda_j \sum_{m=1}^{P_j} \hat{f}_{m,j}^n + \tau\, \hat{s}_j^n, \qquad \text{where} \tag{5}$$

$$\hat{u}_j^n := \frac{1}{|V_j|}\int_{V_j} u(t_n,\mathbf{x})\, dV, \qquad |V_j| := \int_{V_j} 1\, dV, \quad \lambda_j := \frac{\tau}{|V_j|}, \tag{6}$$

$$\hat{s}_j^n := \frac{1}{\tau}\frac{1}{|V_j|}\int_{t_n}^{t_{n+1}}\int_{V_j} s(\mathbf{x}, u(t_n,\mathbf{x}))\, dV dt, \quad \hat{f}_{m,j}^n := \frac{1}{\tau}\int_{t_n}^{t_{n+1}}\int_{\Gamma_{m,j}} \langle \mathbf{f}(u(t,\mathbf{x})), \mathbf{n}_{m,j}(\mathbf{x})\rangle\, d\Gamma dt, \tag{7}$$

i.e., $\hat{u}_j^n$ is the average of the solution over the volume V_j at time level t_n, $\hat{s}_j^n$ is the spatial and temporal average of the source term, $\hat{f}_{m,j}^n$ is the temporal average of the flux in direction of the outer normal $\mathbf{n}_{m,j}$ at the boundary $\Gamma_{j,m}$ of the cell V_j and λ_j is the ratio of the discretization. This means that the average of the solution on the new time level can be calculated from the one on the old time level, the flow over the cell interfaces and the average of the source term. In order to evaluate the flux and the source term, the solution u itself has to be known explicitly. But except for the linear case, we do not have this knowledge. Therefore, the averages $\hat{f}_{m,j}^n$ and $\hat{s}_j^n$ have to be approximated in terms of an approximation $\hat{v}_j^n$ of $\hat{u}_j^n$, i.e., equation (5) reads

$$\hat{v}_j^{n+1} = \hat{v}_j^n - \lambda_j \sum_{m=1}^{P_j} \hat{F}_{m,j}^n + \tau \hat{S}_j^n, \qquad j \in I, \qquad \text{where} \tag{8}$$

$$\hat{F}_{m,j}^n := \hat{F}_m^n\left(\hat{v}_i^n; i \in S_{m,j}\right), \qquad \hat{S}_j^n := s(\hat{x}_j, \hat{v}_j^n), \qquad \hat{\mathbf{x}}_j^n := \frac{1}{|V_j|}\int_{V_j} \mathbf{x}\, dV. \tag{9}$$

Here, $S_{m,j} \subset I$ is a fixed stencil on which the numerical flux $\hat{F}^n_{m,j}$ at the interface $\Gamma_{m,j}$ is calculated. It is commonly assumed that $\hat{F}^n_{m,j}$ is consistent with the flux $\hat{f}^n_{m,j}$, i.e., for constant data $\hat{v}^n_i = c$ the relation $\hat{F}^n_{m,j} = \int_{\Gamma_{m,j}} \langle \mathbf{f}(c), \mathbf{n}_{m,j}(\mathbf{x})\rangle \, d\Gamma$ holds. The numerical fluxes can only be calculated by (9) as long as the stencil is contained in the computational domain. At the boundary we need either further information for $\hat{v}^n_j$ or the numerical fluxes will be based on one–sided stencils. In both cases we have to ensure that the boundary conditions (3) are satisfied. In view of nonlinear boundary conditions, we prefer the definition of physical meaningful data for auxiliary cells. For the numerical fluxes at the boundary Γ we have to apply the boundary conditions (3) themselves and the definition of the averaged flux $\hat{f}^n_{m,j}$, (7).

Schemes of the form (8) are called *finite volume schemes.* They are of great importance from the analytical as well as from the practical point of view. During the last decade they have been applied to numerous practical applications in complex flow fields (cf. $[Y]$). Most of the finite volume schemes have two features in common, firstly solving of Riemann problems at the cell interfaces and secondly the reconstruction of a function by its discrete cell averages to ensure upwinding and higher order discretizations (cf. $[HEOC]$). Thus, the evaluation of the numerical flux is in general very expensive. In order to reduce the costs, Harten developed the strategy of hybrid schemes (cf. $[HC]$), i.e., in smooth flow regions a cheap finite difference scheme is used and in regions with singularities a more expensive upwind scheme is applied. The crucial question is how to distinguish between those regions. For this purpose, Harten developed a multi–resolution technique similar to multigrid techniques (cf. $[H95]$). It is based on a sequence of nested decompositions of Ω. These can successively be constructed either by starting from a given finest decomposition and agglomerating volumes or by refining a given coarsest decomposition. In order to ensure nestedness, we demand

$$V_{k,j} = \bigcup_{l \in D_{k,j}} V_{k+1,l}, \;\; D_{k,j} \subset I_{k+1}, \;\; j \in I_k, \tag{10}$$

i.e., a coarse grid cell is decomposed by $\#D_{k,j}$ fine grid cells. Herein, we have to impose $D_1 \leq \#D_{k,j} \leq D_2$ independently of the level k and the positions j in order to obtain a uniform decomposition and to satisfy certain stability requirements (cf. $[CDP]$). Analogously to (10), we obtain

$$\Gamma_{m,k,j} = \bigcup_{(r,l) \in D_{m,k,j}} \Gamma_{r,k+1,l}, \;\; D_{m,k,j} \subset \{(r,l) \;:\; r \in \{1,\ldots,P_{k,j}\}, \; l \in D_{k,j}\},$$

i.e., a cell interface $\Gamma_{m,k,j}$, $1 \leq m \leq P_{k,j}$ of volume $V_{k,j}$ can be decomposed by $\#D_{m,k,j}$ interfaces corresponding to volumes of the finer grid. According to definition (7), the flux averages in direction of the outer normal to the interface $\Gamma_{m,k,j}$ can now be written as

$$\hat{f}^n_{m,k,j} = \sum_{(r,l) \in D_{m,k,j}} \hat{f}^n_{r,k+1,l} \,. \tag{11}$$

Hence, there exist matrices $\mathbf{R}^{k,l}_{m,r} \in \mathrm{IR}^{|I_k| \times |I_l|}$, $r = 1, \ldots, P_{k,j}$, $0 \leq k \leq l \leq L$, such that

$$\hat{\mathbf{f}}^n_{m,k} = \sum_{r=1}^{P} \mathbf{R}^{k,k+1}_{m,r} \, \hat{\mathbf{f}}^n_{r,k+1} = \sum_{r=1}^{P} \mathbf{R}^{k,L}_{m,r} \, \hat{\mathbf{f}}^n_{r,L} \,, \tag{12}$$

where we introduce the maximal number $P := \max_{0 \leq k \leq L} \max_{j \in I_k} P_{k,j}$ of cell interfaces corresponding to one volume. Definition (7) and equation (12) imply the conservation condition for every level k, i.e.,

$$\Gamma_{m,k,j} = \Gamma_{m',k,j'} \quad \text{for} \quad (m,j) \neq (m',j') \qquad \Longrightarrow \qquad \hat{f}^n_{m,k,j} = -\hat{f}^n_{m',k,j'}. \tag{13}$$

The evolution equations for the averages $\hat{u}_{k,j}$ can now be derived analogously to (5) by

$$\hat{u}_{k,j}^{n+1} = \hat{u}_{k,j}^{n} - \lambda_{k,j} \sum_{m=1}^{P_{k,j}} \hat{f}_{m,k,j}^{n} + \tau \hat{s}_{k,j}^{n}, \quad j \in I_k, \quad k = 0, \ldots, L. \tag{14}$$

For simplicity reasons we assume $P_{k,j} = P$ for all k and j, so that we can write (14) in a vector representation, namely

$$\hat{\mathbf{u}}_k^{n+1} = \hat{\mathbf{u}}_k^n \; - \; \mathbf{\Lambda}_k \sum_{m=1}^{P} \hat{\mathbf{f}}_{m,k}^n \; + \; \tau \, \hat{\mathbf{s}}_k^n, \qquad \text{where} \tag{15}$$

$$\hat{\mathbf{u}}_k^n = \left(\hat{u}_{k,j}^n\right)_{j\in I_k}, \; \mathbf{\Lambda}_k = \operatorname{diag}\left(\{\lambda_{k,j}\}_{j\in I_k}\right), \; \hat{\mathbf{f}}_{m,k}^n = \left(\hat{f}_{m,k,j}^n\right)_{j\in I_k}, \; \hat{\mathbf{s}}_k^n = \left(\hat{s}_{k,j}^n\right)_{j\in I_k}.$$

Herein, the fluxes as well as the source terms are defined according to (7). In the following, the exact averages $\hat{u}_{k,j}^n$ will be approximated by $\hat{v}_{k,j}^n$.

The main idea of Harten's concept is to determine a linear relation between the approximations $\hat{\mathbf{v}}_k^n \in \mathrm{IR}^{N_k}$ and $\hat{\mathbf{v}}_{k+1}^n \in \mathrm{IR}^{N_{k+1}}$ of two neighboring levels, where we denote by N_k the finite number of elements of I_k. For this purpose, additional information in term of a vector $\mathbf{d}_k^n \in \mathrm{IR}^{N_{k+1}-N_k}$ has to be added to the vector $\hat{\mathbf{v}}_k^n$ in order to obtain $\hat{\mathbf{v}}_{k+1}^n$. The quantities $d_{k,j}^n$ can be interpreted as detailed information between the coarse grid k and the fine grid $k+1$. On level $k+1$ we have N_{k+1} unknowns, whereas there are only N_k unknowns available on level k. Hence, we need $N_{k+1} - N_k$ additional information in order to reconstruct the information on the finer level by the data of the coarse level. One possible reconstruction technique is the interpolation of the coarse grid data and the evaluation of the interpolation function at the additional points of the fine grid. These values can be interpreted as a prediction. Of course, an error is introduced by these values, the so–called prediction error, which is denoted by $d_{k,j}$.

The single–scale representation $\hat{v}_L^n$ can successively be replaced by the multi–scale representation

$$\hat{\mathbf{v}}_{MR,L}^n = \left((\mathbf{v}_0^n)^T, (\mathbf{d}_0^n)^T, \ldots, (\mathbf{d}_{L-1}^n)^T\right)^T. \tag{16}$$

Together with (14) a formula can be derived how to calculate the coefficients $d_{k,j}^{n+1}$ of the new time level t_{n+1}. If $|d_{k,j}^n|$ is sufficiently small, then this coefficient is truncated. In this case the numerical flux of level $k+1$ is computed by a linear combination of already calculated fluxes of the coarser level k instead of evaluating the original one, i.e., the computational cost is reduced and thus the computation itself is accelerated. We will see later that there must be a minimal number of truncated coefficients in order to gain a speed up since there is a certain overhead due to the multi–scale transformation.

MULTI–SCALE TRANSFORMATION

In the following we will derive the multi–scale decomposition for the averages $\hat{u}_{k,j}$ of an arbitrary function $u : \Omega \to \mathrm{IR}$ defined on every level $k = 0, \ldots, L$ by

$$\hat{u}_{k,j} := \frac{1}{|V_{k,j}|} \int_{V_{k,j}} u(\mathbf{x}) \, dV, \quad j \in I_k.$$

The main task is to determine a completion of IR^{N_k} to $\mathrm{IR}^{N_{k+1}}$ such that

$$\hat{u}_{k+1,j} = \sum_{r\in I_k} m_{j,r}^k \; \hat{u}_{k,r} + \sum_{r\in J_k} \tilde{m}_{j,r}^k \; d_{k,r}, \quad j \in I_{k+1}, \tag{17}$$

holds and this relation can be inverted, i.e., there exist coefficients $g_{j,r}^k$ and $\tilde{g}_{j,r}^k$ such that

$$\hat{u}_{k,j} = \sum_{r \in I_{k+1}} g^k_{j,r} \; \hat{u}_{k+1,r}, \quad j \in I_k, \tag{18}$$

$$d_{k,j} = \sum_{r \in I_{k+1}} \tilde{g}^k_{j,r} \; \hat{u}_{k+1,r}, \quad j \in J_k, \tag{19}$$

where J_k is the index set corresponding to the coefficients $d_{k,j}$ such that

$$\#J_k = \#I_{k+1} - \#I_k = N_{k+1} - N_k.$$

The coefficients $d_{k,j}$ may be seen as difference information between the data of level k and $k+1$. They can be interpreted as a prediction error as already mentioned above. In matrix–vector representation (17, 18, 19) read

$$\hat{\mathbf{u}}_{k+1} = \mathbf{M}_{k,0} \, \hat{\mathbf{u}}_k + \mathbf{M}_{k,1} \, \mathbf{d}_k, \qquad \hat{\mathbf{u}}_k = \mathbf{G}_{k,0} \, \hat{\mathbf{u}}_{k+1}, \qquad \mathbf{d}_k = \mathbf{G}_{k,1} \, \hat{\mathbf{u}}_{k+1}, \qquad \text{resp.} \tag{20}$$

where

$$\hat{\mathbf{u}}_k := (\hat{u}_{k,j})_{j \in I_k}, \quad \mathbf{d}_k := (d_{k,j})_{j \in J_k},$$

and the prolongation and restriction matrices

$$\begin{aligned} \mathbf{M}_{k,0} &= \left(m^k_{j,r} \right)_{\substack{j \in I_{k+1} \\ r \in I_k}}, & \mathbf{M}_{k,1} &= \left(\tilde{m}^k_{j,r} \right)_{\substack{j \in I_{k+1} \\ r \in J_k}} \\ \mathbf{G}_{k,0} &= \left(g^k_{j,r} \right)_{\substack{j \in I_k \\ r \in I_{k+1}}}, & \mathbf{G}_{k,1} &= \left(\tilde{g}^k_{j,r} \right)_{\substack{j \in J_k \\ r \in I_{k+1}}}. \end{aligned} \tag{21}$$

In order to ensure invertibility between the single–scale and the multi–scale representation these matrices have to satisfy

$$\mathbf{M}_k \mathbf{G}_k = \mathbf{G}_k \mathbf{M}_k = \mathbf{I}, \qquad \text{where} \qquad \mathbf{G}^T_k := \left(\mathbf{G}^T_{k,0}, \mathbf{G}^T_{k,1} \right), \quad \mathbf{M}_k := (\mathbf{M}_{k,0}, \mathbf{M}_{k,1}). \tag{22}$$

By (20) the single–scale representation of $\hat{\mathbf{u}}_L$ can be transformed into the multi–scale representation and vica versa

$$\hat{\mathbf{u}}_{MR,L} := \left(\hat{\mathbf{u}}^T_0, \mathbf{d}^T_0, \ldots, \mathbf{d}^T_{L-1} \right)^T = \mathbf{T}_L \, \hat{\mathbf{u}}_L, \qquad \hat{\mathbf{u}}_L = \mathbf{T}^{-1}_L \, \hat{\mathbf{u}}_{MR,L}, \qquad \text{resp.}$$

introducing the multi–scale transformation $\mathbf{T}_L : \mathrm{IR}^{N_L} \to \mathrm{IR}^{N_L}$ and the inverse multi–scale transformation $\mathbf{T}^{-1}_L : \mathrm{IR}^{N_L} \to \mathrm{IR}^{N_L}$ defined by

$$\mathbf{T}_L := \check{\mathbf{G}}_0 \cdot \ldots \cdot \check{\mathbf{G}}_{L-1}, \qquad \mathbf{T}^{-1}_L := \check{\mathbf{M}}_{L-1} \cdot \ldots \cdot \check{\mathbf{M}}_0, \qquad \text{resp.}$$

Here the matrices $\check{\mathbf{M}}_k$ and $\check{\mathbf{G}}_k$ are given by

$$\check{\mathbf{G}}_k := \begin{pmatrix} \mathbf{G}_k & \mathbf{0} \\ \mathbf{0} & \mathbf{I}_k \end{pmatrix}, \quad \check{\mathbf{M}}_k := \begin{pmatrix} \mathbf{M}_k & \mathbf{0} \\ \mathbf{0} & \mathbf{I}_k \end{pmatrix}, \qquad k = 0 \ldots, L-1,$$

where $\mathbf{I}_k$ denotes the identity matrix in $\mathrm{IR}^{(N_L - N_{k+1}) \times (N_L - N_{k+1})}$.

We want to emphasize that the notation introduced in $[CDP]$ is adapted here.

PROLONGATION AND RESTRICTION

In the previous section a general multi–scale concept has been presented. It is essentially based on the prolongation and restriction matrices which are described in detail in the following.

To our knowledge, there exist two different frameworks in the literature. One possible method has originally been inroduced by Harten $[H96]$ in a more general context than it is applied here. He introduced discretization and reconstruction mappings between a space of functions and a sequence of spaces of coefficient vectors related to different grids. Then he connects two discretization levels by concatenating the discretization and reconstruction operators appropriately. Since the multi–resolution transformation is only based on the relation between two discretizations the space of functions as well as the discretization and reconstruction operators are not really needed. Therefore, they will not be introduced here.

Schröder–Pander and Sonar [SPS] strictly follow this concept when applying it to cell averages on unstructured multi–dimensional grids. They identify the discretization operator with an averaging operator and the reconstruction operator similar to those described later. This leads to a slightly different multi–scale concept for cell averages as derived by Harten [$H95$] in one space dimension.

A different concept examined by Dahmen and the present authors in [DGM] is based on refinable basis functions, where the discrete values $\hat{u}_{k,j}$ and $d_{k,j}$ are identified with the coefficients of a serial expansion with respect to these functions. In this context the multi–scale transformation can be interpreted as a change of basis. The latter is performed by certain matrices that can be identified with prolongation and restriction matrices. This approach offers the promising feature of constructing appropriate basis functions, which lead to *stable* multi–scale transformations, i.e., $\|\mathbf{M}_k\|,\ \|\mathbf{G}_k\| = \mathcal{O}(1),\ k \to \infty$, in (22), which is a crucial property for the stability of the numerical algorithm (cf. [CDP]).

In the following we first present Harten's concept in the framework of the multi–scale transformation, because it is more heuristic and may be easier to understand by the reader who is not familiar with neither of the concepts. Based on this, we give an introduction to the framework of wavelet theory and show the relations to Harten's concept.

CONCEPT OF PREDICTION AND RECONSTRUCTION

First of all, we want to present Harten's method [$H95$] written in matrix–vector notation. By the definition of the cell averages (6) and the assumption of a nested grid hierarchy (10), the matrix $\mathbf{G}_{k,0}$ in (20, 21) has rank N_k and is uniquely determined. In order to derive the matrices $\mathbf{G}_{k,1},\ \mathbf{M}_{k,0},\ \mathbf{M}_{k,1}$ we follow Harten's concept of reconstruction and prediction [$H96$]. Let be $\tilde{\mathbf{u}}_{k+1} \in \mathrm{IR}^{N_{k+1}}$ a linear approximation for $\hat{\mathbf{u}}_{k+1} \in \mathrm{IR}^{N_{k+1}}$ represented in the form

$$\tilde{\mathbf{u}}_{k+1} := \mathbf{R}_k\, \hat{\mathbf{u}}_k, \qquad \mathbf{R}_k \in \mathrm{IR}^{N_{k+1}\times N_k}, \tag{23}$$

such that the *prediction error*

$$\mathbf{e}_{k+1} := \hat{\mathbf{u}}_{k+1} - \tilde{\mathbf{u}}_{k+1} \tag{24}$$

becomes small. Hence, an appropriate choice for the definition of the difference vector $\mathbf{d}_k \in \mathrm{IR}^{N_{k+1}-N_k}$ is

$$\mathbf{d}_k := \mathbf{D}_k\, \mathbf{e}_{k+1}, \qquad \mathbf{D}_k \in \mathrm{IR}^{(N_{k+1}-N_k)\times N_{k+1}}, \tag{25}$$

where $\mathbf{D}_k$ is an arbitrary matrix with rank $N_{k+1} - N_k$. Using (20, 23), (25) yields

$$\mathbf{G}_{k,1} = \mathbf{D}_k - \mathbf{D}_k\, \mathbf{R}_k\, \mathbf{G}_{k,0}. \tag{26}$$

We now assume that the matrix

$$\mathbf{A}_k := \begin{pmatrix} \mathbf{G}_{k,0} \\ \mathbf{D}_k \end{pmatrix} \in \mathrm{IR}^{N_{k+1}\times N_{k+1}} \tag{27}$$

is regular. Considering $\mathbf{A}_k\, \mathbf{e}_{k+1}$, the prediction error can be written as

$$\mathbf{e}_{k+1} = \mathbf{E}_{k,0}\, \hat{\mathbf{u}}_k + \mathbf{E}_{k,1}\, \mathbf{d}_k, \qquad \mathbf{E}_{k,0} \in \mathrm{IR}^{N_{k+1}\times N_k},\ \mathbf{E}_{k,1} \in \mathrm{IR}^{N_{k+1}\times (N_{k+1}-N_k)},$$

where the matrices $\mathbf{E}_{k,0}$, $\mathbf{E}_{k,1}$ are determined by (27, 24, 25, 23), i.e.,

$$\mathbf{E}_{k,0} = \mathbf{A}_k^{-1} \begin{pmatrix} \mathbf{I} - \mathbf{G}_{k,0}\, \mathbf{R}_k \\ \mathbf{0} \end{pmatrix}, \qquad \mathbf{E}_{k,1} = \mathbf{A}_k^{-1} \begin{pmatrix} \mathbf{0} \\ \mathbf{I} \end{pmatrix}.$$

Because of (25), the matrices $\mathbf{E}_{k,0}$, $\mathbf{E}_{k,1}$ are related to $\mathbf{D}_k$ by

$$\mathbf{D}_k\,\mathbf{E}_{k,0} = \mathbf{0}, \qquad \mathbf{D}_k\,\mathbf{E}_{k,1} = \mathbf{I}.$$

By the definition of the prediction error (24) the matrices $\mathbf{M}_{k,0}$, $\mathbf{M}_{k,1}$ turn out to be

$$\mathbf{M}_{k,0} = \mathbf{E}_{k,0} + \mathbf{R}_k, \qquad \mathbf{M}_{k,1} = \mathbf{E}_{k,1},$$

which implies the validity of (22). This fact is related to the regularity of $\mathbf{A}_k$.

In Harten's general multi–scale concept the matrix $\mathbf{E}_{k,0}$ vanishes $[H96, PS]$. This implies $\mathbf{M}_{k,0} = \mathbf{R}_k$ and $\mathbf{D}_k = \mathbf{G}_{k,1}$. It will also be true in the above context, if for every volume $V_{k,j}$ a certain recovery condition holds as we will see later.

In order to determine the coefficients of the prediction (23), we introduce the reconstruction function $R^N_{k,j} : V_{k,j} \to \mathrm{IR}^d$, $j \in I_k$, defined by

$$R^N_{k,j}(\mathbf{x}, \hat{\mathbf{u}}_k) = \sum_{s=0}^{N} \alpha^s_{k,j}(\hat{\mathbf{u}}_k)\,\omega^s_{k,j}(\mathbf{x}), \qquad \mathbf{x} \in V_{k,j}, \tag{28}$$

of the discrete averages $\hat{\mathbf{u}}_k$ (cf. $[BH]$, $[SPS]$, $[GM]$). The functions $\omega^s_{k,j}$ have to be chosen judiciously. The coefficients $\alpha^s_{k,j}$ are determined by the recovery conditions

$$\frac{1}{|V_{k,l}|}\int_{V_{k,l}} R^N_{k,j}(\mathbf{x}, \hat{\mathbf{u}}_k)\,dV \stackrel{!}{=} \hat{u}_{k,l}, \qquad l \in S_{k,j}. \tag{29}$$

Herein, $\tilde{S}_{k,j} := \{i_{k,j,l} \mid l = 0, \ldots, N\}$ is a stencil that is chosen locally for every volume j on level k. In order to ensure the uniqueness of the solution of (29) there must be exactly $N+1$ elements in this set. In general, the index j will be an element of $\tilde{S}_{k,j}$. Otherwise the recovery condition results in an extrapolation.

Substituting (28) into (29) renders a linear system of equations for the coefficients $\alpha^i_{k,j}$. In connection with ENO schemes special reconstruction functions were derived (cf. $[HEOC]$, $[HC]$), $[So]$). They all have in common that they can be written in the form (28), where only the functions $\omega^s_{k,j}$ have to be altered.

We notice that the reconstruction functions $R^N_{k,j}$ are approximations of the function u itself, which is not known. Thus, a quite natural choice for the predictions $\tilde{u}_{k+1,l}$, $l \in D_{k,j}$, is

$$\tilde{u}_{k+1,l} := \frac{1}{|V_{k+1,l}|}\int_{V_{k+1,l}} R^N_{k,j}(\mathbf{x}, \hat{\mathbf{u}}_k)\,dV = \sum_{r \in I_k} a^k_{r,j,l}\,\hat{u}_{k,r}. \tag{30}$$

Herein, the only difference to $\hat{u}_{k+1,l}$ is the substitution of the exact function u by the reconstruction function $R^N_{k,j}$. The coefficients $\alpha^k_{r,j}$ depend linearly on the right hand side, here on $\hat{\mathbf{u}}_k$. Hence, the prediction also depends linearly on $\hat{\mathbf{u}}_k$, i.e., there exist coefficients $a^k_{r,j,l}$, $j, r \in I_k$, $l \in D_{k,j}$, and the prediction can be written in the representation (30). Since we assume $j \in \tilde{S}_{k,j}$ for all $j \in I_k$, the recovery condition yields the identity $\mathbf{G}_{k,0}\,\mathbf{R}_k = \mathbf{I}$ where the matrices are defined by (20, 23) and hence we get $\mathbf{M}_{k,0} = \mathbf{R}_k$ and $\mathbf{E}_{k,0} = \mathbf{0}$, respectively.

CONCEPT OF WAVELETS

The above concept of prediction and reconstruction can also be interpreted in the context of wavelet theory to be described in the following. Here, we follow the framework of Carnicer, Dahmen and Peña $[CDP]$. This concept is based on a sequence of function spaces S_k related to a certain resolution indicated by the index k. Each of the spaces is spanned by a set of basis functions $\Phi_k := (\varphi_{k,j})_{j \in I_k}$, i.e., $S_k := \mathrm{span}\,\Phi_k$, where I_k again is a finite index set, and these spaces are assumed to be nested, i.e., $S_k \subset S_{k+1}$. The nestedness implies the existence of the difference space W_k such that $S_{k+1} = S_k \oplus W_k$. Let Ψ_k be a set of basis functions $\Psi_k := (\psi_{k,j})_{j\in J_k}$ spanning the complement space $W_k := \text{span}\,\Psi_k$. We can now write a function in S_{k+1} in terms of the basis Φ_{k+1} as well as in terms of Φ_k and Ψ_k, i.e., there exist matrices according to (21) such that the two–scale equations

$$\Phi_{k+1}^T = \Phi_k^T\,\mathbf{G}_{k,0} + \Psi_k^T\,\mathbf{G}_{k,1}, \tag{31}$$

$$\Phi_k^T = \Phi_{k+1}^T\,\mathbf{M}_{k,0}, \qquad \Psi_k^T = \Phi_{k+1}^T\,\mathbf{M}_{k,1}, \tag{32}$$

hold, where we interprete the sets of basis functions as vectors. We assume that the identities (22) are satisfied. This guarantees the reversibility of the change of bases.

Now, let $u_{k+1} \in S_{k+1}$, i.e., there exist coefficients $\mathbf{c}_{k+1} \in \mathrm{IR}^{N_{k+1}}$ satisfying

$$u_{k+1} = \Phi_{k+1}^T\,\mathbf{c}_{k+1}\,.$$

On the other hand, there also exist coefficients $\mathbf{c}_k \in \mathrm{IR}^{N_k}$, $\mathbf{d}_k \in \mathrm{IR}^{N_{k+1}-N_k}$ such that

$$u_{k+1} = \Phi_k^T\,\mathbf{c}_k + \Psi_k^T\,\mathbf{d}_k\,.$$

The identity of the two representations, equation (22) and the linear independence of Φ_k and Ψ_k imply the relation between the different coefficients similar to equations (20) where $\hat{\mathbf{u}}_k$ is substituted by $\mathbf{c}_k$.

Up to now, we have only presented the general multi–scale framework. In the following we derive how to apply it to finite volume schemes. To this end, we introduce weighted characteristic functions

$$\tilde{\varphi}_{k,j} := \frac{1}{|V_{k,j}|}\,\chi_{V_{k,j}} \tag{33}$$

where $\{V_{k,j}\}_{j\in I_k}$ is an arbitrary partition of the computational domain Ω. We are now interested in dual basis functions $\varphi_{j,k}$ such that

$$\langle \varphi_{k,l}, \tilde{\varphi}_{k,j}\rangle := \int_\Omega \varphi_{k,l}(\mathbf{x})\,\tilde{\varphi}_{k,j}(\mathbf{x})\,d\mathbf{x} = \delta_{j,l}, \qquad \forall\, j, l \in I_k. \tag{34}$$

In the case of $\Omega = \mathrm{IR}$ and the partition into a uniform grid $V_{k,j} = [2^{-k}\,j, 2^{-k}(j+1)]$, this problem has been solved by Cohen, Daubechies and Feauveau [CDF]. A suitable adaptation for an interval has been performed by Dahmen, Kunoth and Urban [DKU]. This construction can easily be extended to the multi–dimensional Cartesian space by tensor products. Applying regular transformations, this can be mapped to curvilinear spaces (cf. [DGM]). As far as we know, this problem has not been solved for unstructered grids yet. From the orthogonality condition (34) we easily verify

$$c_{k,j} = \langle u_k, \tilde{\varphi}_{k,l}\rangle = \hat{u}_{k,j}, \qquad \forall\, j \in I_k,$$

i.e., the coefficients $c_{k,j}$ of the single–scale representation are just the averages $\hat{u}_{k,j}$ of the function $u_k \in S_k$.

In order to derive the relation to Harten's concept, we define a reconstruction function

$$R_k^N(\mathbf{x}, \hat{\mathbf{u}}_k) := \sum_{j\in I_k} \hat{\mathbf{u}}_{k,j}\,\varphi_{k,j}(\mathbf{x}), \qquad \mathbf{x} \in \Omega.$$

Equations (33,34) guarantee the recovery condition

$$\frac{1}{|V_{k,l}|}\int_{V_{k,l}} R_k^N(\mathbf{x}, \hat{\mathbf{u}}_k)\,dV = \hat{u}_{k,l}, \qquad \forall\, l \in I_k.$$

The prediction function is identified with the reconstruction function and the prediction error is defined accordingly by

$$\tilde{u}_{k+1}(\mathbf{x}) := R_k^N(\mathbf{x}, \hat{\mathbf{u}}_k), \qquad e_{k+1}(\mathbf{x}) := u_{k+1}(\mathbf{x}) - \tilde{u}_{k+1}(\mathbf{x}), \qquad \mathbf{x} \in \Omega\,.$$

Applying the two–scale relations (31,32), we get $\tilde{u}_{k+1} = \Phi_{k+1}^T\,\tilde{\mathbf{u}}_{k+1}$ and $e_{k+1} = \Psi_k^T\,\mathbf{d}_k = \Phi_{k+1}^T\,\mathbf{e}_{k+1}$, where the coefficients are given by $\tilde{\mathbf{u}}_{k+1} := \mathbf{M}_{k,0}\,\hat{\mathbf{u}}_k$ and $\mathbf{e}_{k+1} := \mathbf{M}_{k,1}\,\mathbf{d}_k$. Comparing these representations with those given in the previous section yields

$$\mathbf{E}_{k,0} = \mathbf{0},\ \mathbf{E}_{k,1} = \mathbf{M}_{k,1},\ \mathbf{R}_k = \mathbf{M}_{k,0},\ \mathbf{D}_k = \mathbf{G}_{k,1}.$$

UPDATE OF MULTI–SCALE REPRESENTATION

Now, we apply the multi–scale transformation to the approximations $\hat{\mathbf{v}}_L^n$ of the finite volume scheme (8, 9). According to the previous section, we can calculate the multi–scale representation $\hat{\mathbf{v}}_{MR,L}^n$ in analogy to (16). Since the multi–resolution representation has been derived for a fixed time level, the question arises, how to calculate the multi–resolution representation of the new time level by that of the old time level. According to the multi–scale decomposition (20), we define the multi–scale coefficients of an arbitrary time level n as

$$\hat{\mathbf{v}}_k^n := \mathbf{G}_{k,0}\,\hat{\mathbf{v}}_{k+1}^n \quad \mathbf{d}_k^n := \mathbf{G}_{k,1}\,\hat{\mathbf{v}}_{k+1}^n, \quad k = L-1,\ldots,0, \tag{35}$$

with the single–scale coefficients $\hat{\mathbf{v}}_L^n := \left(v_{L,j}^n\right)_{j\in I_L}$. In order to derive the evolution equations for the mulit–scale coefficients, we start with the finite volume scheme of the finest level given in vector notation by

$$\hat{\mathbf{v}}_L^{n+1} = \hat{\mathbf{v}}_L^n \;-\; \mathbf{\Lambda}_L\hat{\boldsymbol{\delta}}_L^n \;+\; \tau\,\hat{\mathbf{S}}_L^n, \tag{36}$$

where the vector of flux balances is given by $\hat{\boldsymbol{\delta}}_L^n := \sum_{m=1}^P \hat{\mathbf{F}}_{m,L}^n$ and the numerical fluxes and source terms componentwise read for $j \in I_L$

$$\hat{F}_{m,L,j}^n := \hat{F}_m^n\left(\hat{v}_{L,i}^n; i \in S_{m,L,j}\right),\ \hat{S}_{L,j}^n := s(\hat{x}_{L,j}, \hat{v}_{L,j}^n),\ \hat{x}_{L,j}^n := \frac{1}{|V_{L,j}|}\int_{V_{L,j}} \mathbf{x}\,dV. \tag{37}$$

By definition (35) and relation (36), we obtain the multi–scale coefficients of the new time level

$$\hat{\mathbf{v}}_0^{n+1} \;=\; \hat{\mathbf{v}}_0^n \;-\; \mathbf{\Lambda}_0\,\hat{\boldsymbol{\delta}}_0^n \;+\; \tau\,\hat{\mathbf{S}}_0^n, \tag{38}$$

$$\mathbf{d}_k^{n+1} \;=\; \mathbf{d}_k^n \;-\; \mathbf{d}_k^n\left(\hat{\boldsymbol{\delta}}\right) \;+\; \tau\,\mathbf{d}_k^n(\hat{\mathbf{S}}), \qquad k = 0,\ldots,L-1, \tag{39}$$

where the multi–scale coefficients for the flux balances and the source terms turn out to be

$$\mathbf{d}_k^n\left(\hat{\boldsymbol{\delta}}\right) := \mathbf{G}_{k,1}\,\mathbf{\Lambda}_{k+1}\,\hat{\boldsymbol{\delta}}_{k+1}^n, \quad \mathbf{d}_k^n(\hat{\mathbf{S}}) := \mathbf{G}_{k,1}\,\hat{\mathbf{S}}_{k+1}^n \tag{40}$$

and the vector of flux balances as well as the source terms are recursively defined by

$$\hat{\boldsymbol{\delta}}_k^n := \mathbf{\Lambda}_k^{-1}\,\mathbf{G}_{k,0}\,\mathbf{\Lambda}_{k+1}\,\hat{\boldsymbol{\delta}}_{k+1}^n, \quad \hat{\mathbf{S}}_k^n := \mathbf{G}_{k,0}\,\hat{\mathbf{S}}_{k+1}^n \tag{41}$$

initialized on the finest level L by (37). Based on the previous settings, we can now verify

$$\mathbf{M}_{k,0}\,\hat{\mathbf{v}}_k^{n+1} \;+\; \mathbf{M}_{k,1}\,\mathbf{d}_k^{n+1} = \hat{\mathbf{v}}_{k+1}^{n+1}, \quad k = 0,\ldots,L-1,$$

in analogy to (20). This implies that performing one time step in the single–scale representation $\hat{\mathbf{v}}_L^n$ results in the same values $\hat{\mathbf{v}}_L^{n+1}$ as first calculating the multi–scale representation $\hat{\mathbf{v}}_{MR,L}^n$, updating the multi–scale coefficients by (38, 39) and finally decoding $\hat{\mathbf{v}}_{MR,L}^{n+1}$.

At this point, we want to point out that by definition (41) the calculation of $\hat{\mathbf{S}}_0^n$ requires the calculation of *all* $\hat{S}_{L,j}^n$, $j \in I_L$, on the finest level. In principal, this is also true for the flux balances $\hat{\boldsymbol{\delta}}_0^n$, requiring the calculation of *all* numerical fluxes on the finest level.

However, this is not the case if the finite volume scheme (36) on the finest level satisfies a conservation condition analogously to (13) where the exact fluxes $\hat{f}_{m,L,j}$ are to be replaced by the numerical fluxes $\hat{F}_{m,L,j}$. Then, the nestedness of the grid hierarchy (10) implies that the numerical fluxes of level L corresponding to the cell interfaces inside of volume $V_{0,j}$ cancel out, i.e., calculating $\hat{\delta}^n_{0,j}$ requires only the evaluation of numerical fluxes on the finest level corresponding to fine–grid cell interfaces by which the boundary $\partial V_{0,j}$ is composed. Consequently, for calculating the flux balances $\hat{\boldsymbol{\delta}}^n_0$ we only have to compute a small number of numerical fluxes on the finest level, i.e., the higher the refinement degree L the less the number of numerical fluxes. This is the starting point for the acceleration of the underlying finite volume scheme, which is based on the fact, that not all numerical fluxes of the finest level have to be calculated.

In analogy to (11), we can introduce numerical fluxes of level $0 \le k \le L-1$ by

$$\hat{\mathbf{F}}^n_{m,k} = \sum_{r=1}^{P} \mathbf{R}^{k,k+1}_{m,r}\ \hat{\mathbf{F}}^n_{r,k+1} = \sum_{r=1}^{P} \mathbf{R}^{k,L}_{m,r}\ \hat{\mathbf{F}}^n_{r,L},\ k = 0, \ldots, L-1. \tag{42}$$

From the nestedness of the grid hierarchy (10) as well as the conservation condition for the numerical fluxes of the finest level, we conclude

$$\hat{\boldsymbol{\delta}}^n_k = \sum_{m=1}^{P} \hat{\mathbf{F}}^n_{m,k}.$$

Hence, calculating $\hat{\mathbf{v}}^{n+1}_k,\ 0 \le k \le L-1$, according to definition (35) can be interpreted as applying a finite volume scheme to the averages of level k with numerical fluxes and source terms given by (41, 42). But the latter have to be calculated applying the data $\hat{\mathbf{v}}^n_L$ of the finest level.

In view of the truncation process described in the subsequent section we want to rewrite $\mathbf{d}^n_k\left(\hat{\boldsymbol{\delta}}\right)$. To this end, we choose for any $j \in I_k,\ k = 0, \ldots, L-1$, an element $l_{k,j} \in D_{k,j}$. Introducing the sets $D^0_k := \{l_{k,j}\ :\ j \in I_k\}$, $D^0_{k,j} := D^0_k \backslash \{l_{k,j}\}$, $D^1_k := I_{k+1} \backslash D^0_k = \bigcup_{j \in I_k} D^0_{k,j}$, we can rewrite (41) in the form

$$\hat{\delta}^n_{k+1,l_{k,j}} = \hat{\delta}^n_{k,j} - \sum_{s \in D^0_{k,j}} \hat{\delta}^n_{k+1,s}, \quad j \in I_k,\ k = 0, \ldots, L-1.$$

Incorporating this formula in (40) yields

$$\mathbf{d}^n_k\left(\hat{\boldsymbol{\delta}}\right) = \overline{\mathbf{G}}^{k,1}\ \left[\hat{\boldsymbol{\delta}}^{n,1}_{k+1} - \left(\overline{\mathbf{G}}^{k,1}\right)^{-1}\ \tilde{\mathbf{G}}^{k,1}\ \hat{\boldsymbol{\delta}}^n_k\right] =: \overline{\mathbf{G}}^{k,1}\ \left[\hat{\boldsymbol{\delta}}^{n,1}_{k+1} - \tilde{\boldsymbol{\delta}}^{n,1}_{k+1}\right] \tag{43}$$

with the prediction $\tilde{\boldsymbol{\delta}}^{n,1}_{k+1}$ of the flux balances and the matrices $\overline{\mathbf{G}}^{k,1}$, $\tilde{\mathbf{G}}^{k,1}$ given by the coefficients $\overline{g}^{k,1}_{j,r} := g^{k,1}_{j,r}\lambda_{k+1,r} + \tilde{g}^{k,1}_{j,l_{k,m}}$ for $j \in J_k,\ r \in D^1_k$ with $r \in D^0_{k,m},\ m \in I_k$ and $\tilde{g}^{k,1}_{j,r} := -g^{k,1}_{j,r}\lambda_{k+1,r}$ for $j \in J_k,\ r \in D^0_k$. The restricted vector of flux balances is defined by $\hat{\delta}^{n,1}_{k+1,r} := \hat{\delta}^n_{k+1,r},\ r \in D^1_k$. The regularity of $\overline{\mathbf{G}}^{k,1}$ follows from (22), an appropriate enumeration of the columns and a block LU decomposition. Then $\overline{\mathbf{G}}^{k,1}$ turns out to be a Schur complement. In the literature, the matrix is frequently chosen to be a diagonal matrix (cf. $[H95, H96, GM]$).

THRESH–HOLDING

The main objective of the multi–scale transformation applied to conservation laws is the acceleration of the computation. Harten's ansatz is based on the reduction of numerical flux evaluations. Instead of an expensive approximation to the flux based on upwind strategies and solving of Riemann problems a finite difference formula is used in those parts of the flow field where the solution is smooth. This leads to a hybrid scheme.

Here, we follow the original idea of Harten (cf. $[H95]$). This is essentially based on the finite speed of propagation which is characteristic for hyperbolic problems. It can also be applied to convection–diffusion problems as long as convection dominates the problem. A modification taking diffusive effects into account is given in $[B]$.

The concept is based on the idea that coefficients below a certain tolerance can be neglected such that the error produced by this truncation can be controlled. We only take coefficients $d^n_{k,j}$ with $|d^n_{k,j}| > \epsilon_k$ for $\epsilon_k := \epsilon_L/2^{L-k}$, $k = 0, \ldots, L-1$, into account. The remaining coefficients are truncated by setting them to 0. This results in a modified vector $\tilde{\mathbf{v}}^n_{MR,L}$. The error in the single–scale representation can be controlled by

$$\|\hat{\mathbf{v}}^n_L - \tilde{\mathbf{v}}^n_L\|_{1,L} = \|\mathbf{T}^{-1}_L \left(\hat{\mathbf{v}}^n_{MR,L} - \tilde{\mathbf{v}}^n_{MR,L}\right)\|_{h,L} := \sum_{j \in I_L} |V_{L,j}|\, |\hat{\mathbf{v}}^n_{L,j} - \tilde{\mathbf{v}}^n_{L,j}| \leq C\, \epsilon_L,$$

where C is a constant independent of L. Now, we define the set of significant indices of time level n by

$$\mathcal{D}^n := \left\{(k,j) \;:\; k = 0, \ldots, L-1,\ j \in I_k,\ \exists\, r \in D^0_{k,j} \text{ such that } |d^n_{k,r}| > \epsilon_k,\ \right\}.$$

Unfortunately, it is not possible to determine $\mathcal{D}^{n+1}$ without the knowledge of $\hat{\mathbf{v}}^{n+1}_{MR,L}$. But according to the finite speed of propagation we can calculate an approximative set $\tilde{\mathcal{D}}^{n+1} \supset \mathcal{D}^n \cup \mathcal{D}^{n+1}$ by

$$\begin{aligned} &\exists\, r \in D^0_{k,j} \text{ such that } |d^n_{k,r}| > \epsilon_k \;\Rightarrow \\ &(k,s) \in \tilde{\mathcal{D}}^{n+1} \;\text{ for all } s \in I_k \text{ such that } V_{k,s} \text{ is a neighbor of } V_{k,j} \text{ or } s = j. \end{aligned} \tag{44}$$

Furthermore, there must be the possibility that a coarser level influences the next finer one, i. e.

$$\begin{aligned} &\exists\, r \in D^0_{k,j} \text{ such that } |d^n_{k,r}| > \epsilon_k \;\Rightarrow \\ &(k+1,s) \in \tilde{\mathcal{D}}^{n+1}, \;\text{ for all } s \in I_{k+1} \text{ such that } V_{k+1,s} \subset V_{k,j}. \end{aligned} \tag{45}$$

The reason for this is that *all* coefficients of a certain level, say k_0, may be truncated but again needed after some time because a discontinuity has developed. Applying (44) without (45), the coefficients needed on level k_0 would not be indicated as significant again. However, the combination of both rules does so. This is the reason why Harten follows both instructions in $[H95]$, whereas we made the experience that this case practically does not occur. Then, (45) just increases the number of significant indices on level $k_0 + 1$.

In order to determine the smooth part of the solution, the set $\tilde{\mathcal{D}}^{n+1}$ is helpful. If $(k,j) \notin \tilde{\mathcal{D}}^{n+1}$, the flux balance $\hat{\delta}^{n,1}_{k+1,r}$ can be replaced by the prediction $\tilde{\delta}^{n,1}_{k+1,r}$ for all $r \in D^0_{k,j}$. In this case, equations (39, 43) reduce to

$$d^n_{k,j}\left(\hat{\boldsymbol{\delta}}\right) = 0, \quad \hat{\delta}^n_{k+1,r} = \tilde{\delta}^{n,1}_{k+1,r}, \quad d^{n+1}_{k,r} = 0 \quad \forall\, r \in D^0_{k,j}$$

where the flux balances of level $k+1$ are calculated from already known flux balances on level k. Hence, *not* all fluxes $\hat{F}^n_{m,k+1,j}$, $j \in I_{k+1}$, have to be calculated on level $k+1$. This fact will significantly reduce the computational costs, especially when the evaluation of the numerical flux is very expensive.

In order to ensure a high truncation rate, we demand that the multi–scale coefficients will vanish in the case of homogeneous single–scale data, i.e.,

$$\mathbf{u}_{k+1} = c\,\mathbf{1} \Leftrightarrow \mathbf{u}_k = c\,\mathbf{1}, \quad \mathbf{d}_k = \mathbf{0},$$

for $k = 0, \ldots, L-1$. A sufficient condition is $\mathbf{G}_{k,0}\,\mathbf{1} = \mathbf{1}$, $\mathbf{G}_{k,1}\,\mathbf{1} = \mathbf{0}$, i.e., the multi–scale transformation has zero order vanishing moments and the prediction error is of first order. In practice, the truncation rate turns out to increase, when there are higher vanishing moments in the context of wavelet theory and the predicition error is of higher order in the context of prediction and reconstruction, respectively.

APPLICATION

In our numerical experiments we consider a shock–focussing problem. This is initialized by piecewise constant data $\mathbf{u}_I$, $\mathbf{u}_O$ inside and outside a sphere with radius R_{sph}. Assuming a lower pressure inside the sphere, a shock wave followed by a contact discontinuity runs towards the center of the sphere whereas a rarefaction wave moves in the opposite direction. At a certain time $T > 0$ the shock wave focusses in the center and is reflected. The resulting flow field is rotational symmetric. Since we neglect viscosity and heat conduction, the problem is appropriately modelled by the three–dimensional Euler equations in spherical coordinates. Herein, the tangential velocity components vanish because of rotational symmetry. The resulting equations in differential form for mass density ρ [kg/m^3], radial velocity component v_r [m/s] and mass specific total energy E [J/m^3] thus read

$$\frac{\partial\,\mathbf{u}(t,r)}{\partial\,t} + \frac{\partial\,\mathbf{f}(\mathbf{u}(t,r))}{\partial\,r} = \mathbf{s}(r,\mathbf{u}(t,r)),$$

where the vector of conservative quantities $\mathbf{u}$, the flux $\mathbf{f}$ and the source $\mathbf{s}$ are given by

$$\mathbf{u} = \begin{pmatrix} \rho \\ \rho\, v_r \\ \rho\, E \end{pmatrix}, \quad \mathbf{f}(\mathbf{u}) = \begin{pmatrix} \rho\, v_r \\ \rho\, v_r^2 + p \\ v_r\,(\rho\, E + p) \end{pmatrix}, \quad \mathbf{s}(r,\mathbf{u}) = -\frac{1}{r}\begin{pmatrix} \rho\, v_r \\ \rho\, v_r^2 \\ v_r\,(\rho\, E + p) \end{pmatrix}.$$

The system has to be closed by an equation of state for the pressure p. Assuming a perfect gas, we obtain

$$p = (\gamma - 1)\rho\left(E - \frac{1}{2}v_r^2\right),$$

with the constant ratio of specific heats at constant pressure and volume, respectively, $\gamma = c_p/c_V$. In our calculations we choose $\gamma = 1.4$ for two–atomic gas.

The following test configuration has been considered

$$\mathbf{u}(t,x) = \begin{cases} \mathbf{u}_I & , \quad 0 \le x < R_{sph}, \\ \mathbf{u}_O & , \quad R_{sph} \le x \le 2\,R_{sph}, \end{cases}$$

where the radius is chosen to be $R_{sph} = 0.05$ [m] and the initial data for the conservative quantities are given by

$$\mathbf{u}_I = (1.251,\ 0,\ 253250)^T, \quad \mathbf{u}_O = (2.502,\ 0,\ 506500)^T.$$

The corresponding pressures are $p_I = 1013$ $[hPa]$, $p_O = 2026$ $[hPa]$.

At the left boundary we apply reflecting boundary conditions, whereas we assume vanishing von Neumann conditions at the right boundary.

A parameter study with respect to L has been performed. The following parameters are chosen:

- finite volume scheme: ENO–scheme of 2nd order with reconstruction via primitive function of characteristic variables and exact Riemann solver (cf. $[HEOC]$),
- CFL–number: 0.4,

L	N_L	ϵ	N_F	η	T_{MS}	T_{FVV}	θ
3	200	0.025	201	1.00	39 s	35 s	0.90
4	400	0.05	331	0.83	130 s	130 s	1.00
5	800	0.1	415	0.52	420 s	520 s	1.24
6	1600	0.2	453	0.28	1200 s	2200 s	1.83
7	3200	0.4	458	0.14	4500 s	8800 s	1.96
8	6400	0.8	484	0.08	16000 s	35000 s	2.19

Table 1: Computations for multi–scale scheme und original finite volume scheme

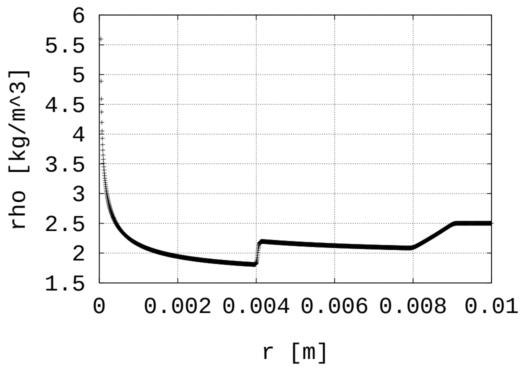

Figure 1: Density

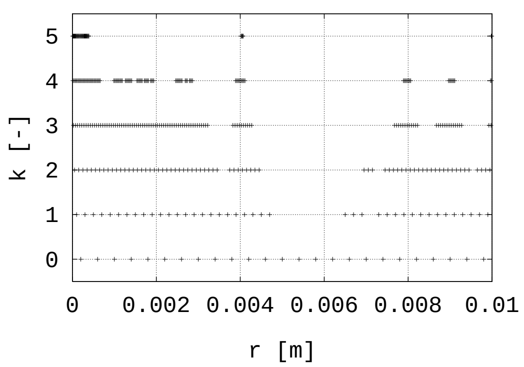

Figure 2: Significant multi–scale coefficients

- multi–scale transformation: polynomial reconstruction of degree 4 with boundary adaptation according to $[GM]$,
- multi–scale scheme: $L = 3, 4, 5, 6, 7, 8$, $N_0 = 25$, $N_L = 25 \cdot 2^L$, with thresh–hold parameter $\epsilon = 0.025 \cdot 2^{L-3}$.

In Tab. 1 some quantities are collected demonstrating the increase of efficiency of the multi–scale strategy:

- maximum number N_F of numerical flux evaluations per time step for the mutli–scale scheme, i.e., $\max\{|\tilde{\mathcal{D}}_{n+1}| + N_0 + 1 \mid 0 \leq n \leq N_T\}$ where N_T is the number of time steps, in contrast to $N_L + 1$ numerical flux evaluations for the finite volume scheme,
- computational time T_{MS} for the multi–scale scheme and T_{FVV} for the basic finite volume scheme without multi–resolution,
- ratios $\eta = N_F/N_L + 1$ and $\theta = T_{FVV}/T_{MS}$ as measures for efficiency.

We notice that a reduction of flux evaluations η corresponds to an acceleration θ of the computation. However, these are not correlated linearly. This is caused by the additional effort for calculating the multi–scale transformation increasing with $\mathcal{O}(N_L)$.

As an example, we present the results for $L = 6$ on the finest level. In Fig. 1 the density is plotted at time $T = 1.19084 \cdot 10^{-5}$ [s]. There is no difference visible between the data corresponding to the finite volume scheme and the multi–scale scheme. The spatial distribution of the corresponding significant multi–scale coefficients is shown in Fig. 2. A significant index (k, j) corresponds to $((2j + 1)/N_{k+1}, k)$. We notice that the shock wave and the contact discontinuity have to be resolved by the finest grid. Also for the rarefaction wave, which is continuous but not continuously differentiable, we have to access to the second finest level. In contrast to this, the smooth part of the solution is characterized by the fact that only multi–scale coefficients of the lowest level are involved.

CONCLUSION

We investigate an acceleration technique for finite volume schemes developed by Harten. There are three ingrediences needed in order to reduce computational costs:

- multi–scale representation of discrete data;
- thresh–holding techniques similar to those in data compression;
- update strategy of the time–dependent multiscale representation.

Increasing efficiency is achieved by substituting expensive numerical flux evaluations by cheap interpolation formulas, where the switching procedure is based on multi–scale representation of discrete averages and thresh-holding techniques.

In our investigations we introduce a multi–scale concept for discrete data. This is essentially based on reconstruction and interpolation operators which relate information on different scales and describe a change of basis. In terms of these operators, Harten's general framework for arbitrary discrete data can be written in a very compressed form. It also enables us to apply the wavelet theory — especially bi–orthogonal wavelets — in this context. We want to emphasize that this concept does not depend on the underlying discretization of the computational domain. The multi–resolution representation is reduced by a thresh–holding technique taking the finite speed of propagation into account which is characteristic for hyperbolic problems. In a final step, the compressed multi–scale data are updated from one time level to the next. Here, we are able to present a genuinely multi–dimensional strategy. This is different to those of Harten's one–dimensional technique (cf. [$H96$]), Sjögreen's straight forward extension by dimensionally splitting (cf. [S]) and the tensor product ansatz of Bihari and Harten (cf. [BH]).

The efficiency of the concept is demonstrated by an application to a physical meaningful test configuration. A speed up of about 2 is achieved. But we believe that a much higher ratio is possible, if the computational overhead caused by the multi–scale transformation can be reduced. To this objective, adaptive memory allocation strategies must be developed, in order to restrict the memory by the number of data that is required to guarantee a certain resolution of the approximation instead of the number of data on the finest level. Therefore, Harten's concept which starts from the finest grid has to be altered. Instead of calculating the numerical fluxes to the data of the finest level we have to use data on the coarser level. However, first investigations showed that oscillations occur near discontinuities when applying the strategy to an explicit scheme. But we are hopeful to overcome these problems by an implicit strategy.

In the end, we want to remark that up to now no thresh–holding is applied to the multi–scale representation of the source terms. Since those terms are averages in the space–time continuum, Harten's fundamental idea of evaluating the originally fluxes and sources on the coarsest level to the data on the finest level results in evaluating all sources on the finest level, i.e., no thresh–holding is possible. This problem is related to the evaluation of nonlinear functions with respect to arguments in multi–scale representation, which is not solved yet.

ACKNOWLEDGEMENT

The authors are very grateful to Wolfgang Dahmen for many inspiring discussions. They also would like to thank Karsten Urban for helpful remarks concerning the presentation.

REFERENCES

[B] Bihari, B . L.: "Multi–resolution Schemes for Conservation Laws with Viscosity", J. Comp. Phys., 123, 1996, pp. 207–225.

[BH] Bihari, B . L., Harten, A.: "Multi–resolution Schemes for the Numerical Solution of 2D Conservation Laws I", SIAM J. SCI. Statist. Comput., to appear.

[CDF] Cohen, A., Daubechies, I., Feauveau, J. –C.: "Biorthogonal Bases of compactly supported Wavelets", Comm. Pure Appl. Math., Vol. 45, 1992, pp. 485–560.

[CDP] Carnicer, J. M., Dahmen, W., Peña, J. M.: "Local Decomposition of Refinable Spaces", Appl. Comp. Harm. Anal., 3, 1996, pp. 127–153.

[DGM] Dahmen, W., Gottschlich–Müller, B., Müller, S.: "A Multi–resolution Scheme based on Bi–orthogonal Wavelets for Conservation Laws", in preparation.

[DKU] Dahmen, W., Kunoth, A., Urban, K.: "Biorthogonal Spline–Wavelets on the Interval — Stability and Moment Conditions", Internal Report No. 129, Institut für Geometrie und Praktische Mathematik, RWTH Aachen, 1996.

[GM] Gottschlich–Müller, B., Müller, S.: "Multi–scale Concept for Conservation Laws", Internal Report No. 128, Institut für Geometrie und Praktische Mathematik, RWTH Aachen, 1996.

[$HEOC$] Harten, A., Engquist, B., Osher, S., Chakravarthy, S. R.: "Uniformly high order accurate Essentially Non–Oscillatory Schemes III", J. Comp. Phys., 71, 1987, pp. 231–303.

[HC] Harten, A., Chakravarthy, S. R.: "Multidimensional ENO Schemes for General Geometries", ICASE Report, NASA Contractor Report NAS1–18605.

[$H95$] Harten, A.: "Multi–resolution Algorithms for the Numerical Solution of Hyperbolic Conservation Laws", Comm. Pure Appl. Math., Vol. 48, No. 12, 1995, pp. 1305–1342.

[$H96$] Harten, A.: "Multi–resolution Representation of Data: A General Framework", SIAM J. Numer. Anal., 33, 1996, pp. 1205–1256.

[L] LeVeque, R.: "Numerical Methods for Conservation Laws", Birkhäuser, 1992.

[S] Sjögreen, B.: "Numerical experiments with the Multiresolution Scheme for the Compressible Euler Equations", J. Comp. Phys., 117, 1995, pp. 251–261.

[So] Sonar, Th.: "Multivariate Rekonstruktionsverfahren zur numerischen Berechnung hyperbolischer Erhaltungsgleichungen", Habilitationsschrift, TH Darmstadt, 1995.

[SPS] Schröder–Pander, F., Sonar, Th.: "Preliminary Investigations on Multiresolution Analysis on Unstructured Grids", DLR Forschungsbericht IB 223–95 A 36, 1995.

[Y] Yee, H. C.: "A class of High–Resolution Explicit and Implicit Shock–Capturing Methods", VKI Lecture Series 04–1989.